Molecular Crystals and Liquid Crystals Science and Technology. Section A. Molecular Crystals and Liquid Crystals

Publication details, including instructions for authors and subscription information:
http://www.tandfonline.com/loi/gmcl19

Talbot Assisted Pattern Formation in a Liquid Crystal Film with Single Feedback Mirror

Enrico Santamato [a], Ernesto Ciaramella [b] & Mario Tamburrini [b]

[a] Dipartimento di Scienze Fisiche, Università di Napoli, Pad.20 Mostra d'Oltremare, 80125, Napoli, Italy

[b] Fondazione Ugo Bordoni, via B. Castiglione 59, 00142, Roma, Italy

Version of record first published: 24 Sep 2006.

To cite this article: Enrico Santamato , Ernesto Ciaramella & Mario Tamburrini (1994): Talbot Assisted Pattern Formation in a Liquid Crystal Film with Single Feedback Mirror, Molecular Crystals and Liquid Crystals Science and Technology. Section A. Molecular Crystals and Liquid Crystals, 251:1, 127-143

To link to this article: http://dx.doi.org/10.1080/10587259408027198

Mol. Cryst. Liq. Cryst. 1994, Vol. 251, pp. 127–143
Reprints available directly from the publisher
Photocopying permitted by license only

Printed in the United States of America

TALBOT ASSISTED PATTERN FORMATION IN A LIQUID CRYSTAL FILM WITH SINGLE FEEDBACK MIRROR

ENRICO SANTAMATO
Dipartimento di Scienze Fisiche, Università di Napoli, Pad.20 Mostra d'Oltremare, 80125 Napoli, Italy,

ERNESTO CIARAMELLA, MARIO TAMBURRINI
Fondazione Ugo Bordoni, via B.Castiglione 59, 00142 Roma, Italy

Abstract We investigated experimentally the spontaneous formation of regular patterns of filaments in a laser beam traversing a thin liquid crystal film placed in front of a single mirror. The transistion from hexagonal to roll-like pattern was experimentally investigated as a function of the laser beam incidence angle and mirror distance. Square patterns were observed by inserting a thin slit behind the mirror. Our observations strongly support a simple model for pattern formation based on Talbot effect.

INTRODUCTION

The spontaneous formation of transverse spatial structures during beam propagation in nonlinear optical media has recently received great attention [1]. Potential applications are image recognition and optical computing, but there is also a fundamental interest in the phenomenon, because regular structures are formed spontaneously from noise in dissipative systems. The phenomenon is known as self-organization. Spontaneous growing of spatial transverse structures in laser beams was reported when highly nonlinear Kerr media are inserted in a Fabry-Perot cavity [2]. Even more complicate spatial structures as defects or vortex have been observed when a degenerate four wave mixing with gain is realized in a highly nonlinear Kerr material (namely a BSO photorefractive crystal) inserted in a ring cavity [3].

The nonlinear Fabry-Perot scheme is complicate, because of the coherence requirements and of the complexity of the mechanism providing the optical feedback, requiring a very careful alignment optimization. For this reasons simpler systems, based on one backreflecting mirror [4] or even without external optical feedback at all are of great interest. Nontrivial spatial structures (two-dimensional dark-solitons) with no external feedback were observed in sodium vapors near the D_2 resonance, where the gas behaves as a negative (de-focusing) optical Kerr medium [5]. These structures, however, do not form spontaneously from noise, but must be initialized by some "seed", made, e.g., by making the incident laser beam to pass through a wire mesh. The possibility of forming highly structured hexagonal patterns from noise using just a single backreflecting mirror was proved both theoretically [1,6,4] and experimentally in a thin nematic liquid crystal film [7,8,9] and also in $KNbO_3$ crystal [10].

In this paper we present some recent results on pattern formation obtained by retroreflecting a cw argon laser beam onto a film of homeotropically aligned nematic liquid crystal. These results include the study of hexagonal pattern formation with the backreflecting mirror placed at *negative* distance from the nematic cell [11], the transition from hexagons to rolls when the overall cylindrical symmetry around the beam propagation direction is broken, and the observation of square patterns when the system is fed with a suitable seed [12], confirming recent results obtained by numerical simulations [14].

FIRTH'S MODEL

Consider a thin slice of nonlinear optical medium, characterized by a nonlocal Kerr-like response to the optical field. When a laser beam traverses the slice, it suffers a nonlinear phase change φ proportional to the beam intensity I. We assume a nonlocal Kerr response, due to diffusion in the medium. The relationship relating the nonlinear phase change to the laser intensity is therefore of the form of a diffusion equation, viz.

$$\tau\frac{\partial\varphi}{\partial t} - l_x^2\frac{\partial^2\varphi}{\partial x^2} - l_y^2\frac{\partial^2\varphi}{\partial y^2} + \varphi = aI, \tag{1}$$

where τ is the response time of the medium and, for greater generality, we assumed different diffusion lengths l_x and l_y along the x- and y- directions in the plane transverse to the beam propagation axis. The medium is assumed to be perfectly transparent and very thin so that self-focusing inside the the medium is negligible. The intensity $I = I(x, y)$ is therefore independent of the z-coordinate. At steady state and with negligible diffusion, Eq.(1) reduces to the usual local proportionality between the nonlinear phase change φ and the beam intensity I. In Firth's model [1,6,4] it is assumed that the intensity I in Eq.(1) is made of the sum of the intensity profile I_0 of the incident beam and the intensity profile I_1 of the beam backreflected from the plane mirror, located at distance d from the nonlinear slice. No interference occurs between the two counterpropagating waves. The optical field $\bar{u}_0$ produced by the beam inciding onto the nonlinear slice is assumed to have constant phase $\bar{\psi}$ in the transverse plane, viz.

$$\bar{u}_0(x, y) = \sqrt{I_0(x, y)} e^{i\bar{\psi}}. \tag{2}$$

Then, the optical field u_0 at the exit of the nonlinear film is given by

$$u_0(x, y) = \sqrt{I_0(x, y)} e^{i[\bar{\psi} + \psi_0 + \varphi(x,y)]}, \tag{3}$$

where ψ_0 and $\varphi(x, y)$ are the linear and the nonlinear phase shifts due to the beam propagation through the nonlinear film. Being $2d$ the round-trip distance covered by the beam going to and from the plane mirror, the field u_1 reflected back into the film is given by Fresnel formula

$$\begin{aligned} u_1(x, y; \varphi) &= \sqrt{I_1(x, y; \varphi)} e^{i\psi_1(x,y;\varphi)} \\ &= \frac{-i}{2\lambda d} e^{\frac{4\pi i d}{\lambda}} R \iint_{-\infty}^{+\infty} dx'\, dy'\, u_0(x', y') e^{\frac{i\pi[(x-x')^2 + (y-y')^2]}{2\lambda d}}, \end{aligned} \tag{4}$$

where u_0 is given by Eq.(2), d is the mirror-to-cell distance, R is the mirror reflectivity, and λ is the optical wavelength. In Eq.(4) the functional dependence of u_1 on the nonlinear phase change φ is explicitly indicated[1]. The total intensity I appearing on the right of Eq.(1) is therefore given by $I(x, y; \varphi) = I_0(x, y) + I_1(x, y; \varphi)$, with $I_1 = |u_1|^2$, so that Eq.(1) is transformed into a nonlinear integro-differential

[1] Because of the sample transparency, the intensity profile $I_0(x, y)$ of the incident beam remains fixed

equation for the nonlinear transverse phase change $\varphi(x,y)$. This equation was solved numerically by Firth et al. [1,6,4], who showed that, in the plane-wave approximation (I_0 =const.) and above a critical threshold I_{th} in the incident wave intensity I_0, two-dimensional periodic solutions $\varphi(x,y)$ with bright filaments in a regular hexagonal lattice become stable. In the plane wave approximation Eq.(1) has the trivial uniform solution $\varphi = (1+R)aI_0$. The stability of this solution can be investigated analytically by a standard linear stability analysis. It is found that this solution becomes unstable when the intensity I_0 of the incident plane wave reaches the threshold value

$$I_{th} = \frac{1 + K_{th}^2 l^2}{2aR\sin(\frac{K_{th}^2 d\lambda}{2\pi})}, \tag{5}$$

where the lattice spatial frequency K_{th} of $\varphi(x,y)$ at threshold is given by the root of the trascendental equation

$$\tan(\frac{K_{th}^2 d\lambda}{2\pi}) = \frac{K_{th}^2 d\lambda}{2\pi} + \frac{d\lambda}{2\pi l^2} \tag{6}$$

and $l = \max(l_x, l_y)$.

We conclude this section by noting that what is actually observed in the experiments is not the phase $\varphi(x,y)$ itself, but the intensity $I_1(x,y) = |u_1(x,y)|^2$ of the reflected field at the sample, as given by Eq.(4). Once $\varphi(x,y)$ is known, the field $u_1(x,y)$ can be evaluated from Eq.(4). In the plane wave approximation (beam waist w much larger than the spatial period $\Lambda = 2\pi/K$ of the periodic phase pattern), $u_1(x,y)$ is simply obtained, apart from unessential constant phase factors, from Fresnel propagation of $e^{i\varphi(x,y)}$ over the round-trip distance $2d$.

TALBOT APPROACH

The occurrence of periodic structures in the phase (and intensity) of the reflected beam after having traversed the nonlinear medium can be understood by using the well known Talbot effect of Fourier optics [15]. Let us assume that, after having passed through the nonlinear medium, a plane wave gains small amount of *periodic* transverse phase modulation (PM). Talbot fractional imaging causes the periodic phase modulation of the wave to be changed into amplitude modulation (AM) by

free propagation in vacuum. More precisely, if the initial wave is weakly phase modulated with a phase grating having spatial period Λ, after free propagation over a distance

$$l_T = \frac{2\Lambda^2}{\lambda} \tag{7}$$

the wave phase modulation is restored so that initial field at $z = 0$ is self-reproduced at planes $z_m = ml_T$, with positive integer m. The length l_T given by Eq.(7) is called Talbot self-imaging length. This remarkable result is a straightforward property of Fresnel propagator appearing in Eq.(4). A closer inspection into Fresnel integral shows that, after free propagation over a distance $l_T/4$, the initially PM wave is changed into an AM wave. The amplitude modulation of

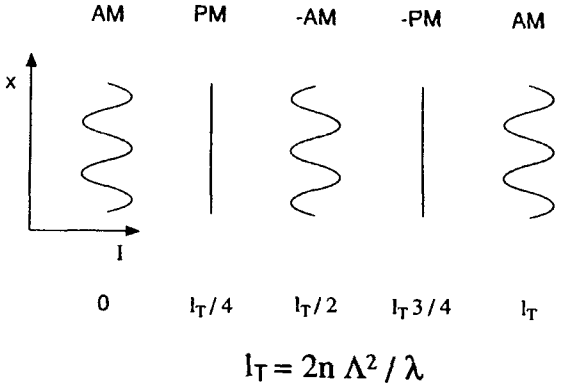

FIGURE 1 Talbot's effect. n is the refractive index of the medium.

the optical field at $z = l_T/4$ is in phase with the phase modulation of the field at $z = 0$. After further propagation of $l_T/4$, the wave becomes again PM, but out of phase with respect to the initial field. Again, at distance $l_T/4$ later, the wave is still AM modulated, but with opposite phase. Eventually, after the distance l_T the initial phase modulation is restored. These passages from PM to AM are shown schematically in Fig.1. Assume now that a mirror is placed at the plane $z = d = l_T/8$. From Fig.1, we see that the field reflected onto the sample is AM

in phase with the phase modulation of the incident wave. Because of the Kerr nonlinearity of the medium, the AM of the reflected wave induces a corresponding phase modulation in the incoming wave tending to enhance the already present spatial modulation. Thus we see that, according to Talbot model, the mirror-to-sample distance d determines the period Λ_T of the spatial phase grating that can suffer positive feedback in the medium, because the following condition must be fulfilled

$$\Lambda_T = \sqrt{\lambda l_T/2} = 2\sqrt{\lambda d}. \tag{8}$$

When the incident laser intensity I is above threshold for self oscillation, a two-dimensional index grating having lattice period given by Eq.(8) is generated in the nonlinear medium.

If perfect cylindrical symmetry is assumed around the z-axis, only three regular lattices characterized by one given lattice constant $K = 2\pi/\Lambda$ can be realized on the (x, y)-plane, namely a ripple, a square or an hexagonal lattice. The hexagonal pattern is preferred to the square and ripple ones, because it requires less energy to be created. In fact, inducing an index change in the medium requires, in general, the expense of some work that must be provided by the incoming light. In the case of liquid crystals, this work is used to reorient the molecules. The index change (and, hence, the local work) is very high only near the vertex of the phase lattice created in the medium, where the light intensity has a local maximum. Therefore, the total energy that the light must provide to the system is roughly proportional to the number of lattice vertices falling in the illuminated area A. This number is A/Λ^2 for squares and $\sqrt{3}A/(2\Lambda^2)$ for hexagons, due to their lower filling factor (note that Λ is the apothem of the hexagonal cell) . Because the comparison must be performed with fixed Λ, hexagons require a lower $\sqrt{3}/2$ times less work. Clearly, ripple patterns have larger high intensity areas and are therefore more energy consuming.

Hexagonal patterns require almost isotropic diffusion in the (x, y)-plane, i.e. $l_x \simeq l_y$. When $l_x >> l_y$, one dimension oscillation prevails and the resulting periodic pattern assumes the form of rolls orthogonal to the x-axis.

THE LIQUID CRYSTAL MEDIUM

Liquid crystals may have a huge optical nonlinearity. The nonlinearity arises from the high degree of electron delocalization in the molecules, the large anisotropy of the molecular structure, and the strong correlation of their motion. In the mesophases, the molecular correlation is so strong and the optical nonlinearity is so large that propagation of laser beams in these materials leads to very unusual, but interesting, effects, that cannot be described by the perturbative approach commonly used in nonlinear optics [16]. Liquid crystals in the mesophases cannot be considered, therefore, as true Kerr optical media. Nevertheless, in some circumstances, they can simulate a medium with huge nonlinear Kerr-like optical nonlinearity. This happens when the following conditions are satisfied:

- light polarization is linear and remains unchanged during the propagation in the medium;
- direction of the light polarization is oblique with respect to the molecular orientation as impressed initially by the anchoring forces at the sample walls;
- light intensity is not too large.

The first condition avoids effects related to the change of the state of the beam polarization as it traverses the medium. The second condition guarantees that the optical torque is nonzero somewhere in the sample even in the limit of very small intensity. This avoids the occurrence of threshold effects as in the Optical Fréedericksz Transition [21,22]. The third condition is required in order to induce a small distortion in the sample and validate the standard perturbative approach used in nonlinear optics. All of these conditions are met in the following experimental geometries

1. homeotropic cell with laser beam at oblique incidence;
2. planar cell with laser at oblique incidence;
3. hybrid cell.

Geometry (3) was used in Ref. 7. Geometry (1) in Refs. 8,9,11,12. All experimental results presented in this work refer to geometry (1). To our knowledge, no experiments have been reported using geometry (2). In all of these geometries only splay-bend distortion is induced in the sample and the molecular director $\boldsymbol{n}$ can be written as $\boldsymbol{n} = (\sin\vartheta, \cos\vartheta, 0)$, where ϑ is the tilt angle with respect to the $\hat{z}$-axis normal to the sample walls (which is different from the z-axis along the beam), because of the oblique incidence. In this work only geometry (1) with strong anchoring at the walls will be considered for a nematic cell of thickness L. Because the light intensity is small, the laser-induced reorientation is small as well, and the torque equation can be linearized for small tilt angle ϑ. Then a straightforward calculation yields

$$-\gamma_1 \frac{\partial \vartheta}{\partial t} + k_{11} \frac{\partial^2 \vartheta}{\partial \hat{x}^2} + k_{22} \frac{\partial^2 \vartheta}{\partial \hat{y}^2} + k_{33} \frac{\partial^2 \vartheta}{\partial \hat{z}^2} - \frac{(n_e^2 - n_o^2)\sin\alpha\cos\alpha}{c n_e^2} I = 0, \tag{9}$$

where γ_1 is the liquid crystal viscous coefficient, k_{11}, k_{22} and k_{33} are the elastic constants for splay, twist and bend deformation, respectively, n_o and n_e are the ordinary and extraordinary refractive indices, α is the beam incidence angle, and, finally, I is the beam intensity. The boundary conditions are $\vartheta(0) = \vartheta(L) = 0$. The nonlinear phase change φ experienced by the extraordinary wave in traversing the medium can be easily evaluated observing that, for small ϑ, we have

$$\varphi = \beta < \vartheta >, \tag{10}$$

with

$$\beta = \left[\frac{2\pi(n_e^2 - n_o^2)L}{n_e^2 \lambda}\right] \sin\alpha, \tag{11}$$

where $< \vartheta >= L^{-1} \int_0^L \vartheta \; d\hat{z}$ and α is the laser incidence angle. The stationary solution of Eq.(9) with boundary conditions $\vartheta(0) = \vartheta(L) = 0$ can be written as

$$\vartheta = 6 < \vartheta > \hat{z}(L - \hat{z})/L^2. \tag{12}$$

Inserting this ϑ-profile into Eq.(9) and using Eqs.(10) and (11) we find that the effective nonlinear Kerr index $< n_2 >$ defined by the relationship $\varphi = 2\pi L n_2 I/\lambda$, is given by

$$n_2 = \frac{(n_e^2 - n_o^2)^2 L^2}{12 c n_e^4 K} \sin^2 \alpha \cos \alpha. \tag{13}$$

We notice that the effective optical Kerr index is proportional to the square of the sample thickness L (the nonlinear phase change is proportional to L^3) and depends also on the beam incidence angle α. A plot of n_2 as a function of the beam incidence angle α is reported in Fig.2 for a 120μm thick $E7$ homeotropic cell. A simple integration of Eq.(9) along $\hat{z}$ yields, after multiplication by β, the

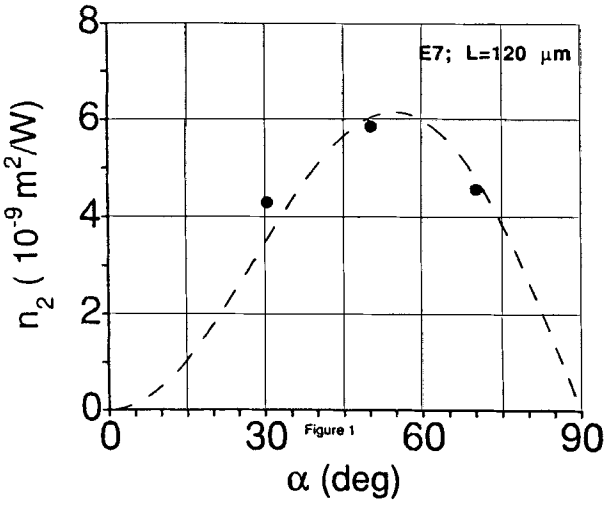

FIGURE 2 Measured effective nonlinear Kerr coefficient n_2 as a function of the beam incidence angle α for a 120μm tick nematic $E7$ homeotropic cell. The measurement was made with a Mac Zehnder interferometer. The dashed curve is the best fist from Eq.(13). The $5CB$ elastic constants were obtained, in the same experiment, as $k_{11} = 12.1\ 10^{-7}$dyne, $k_{22} = 6.55\ 10^{-7}$ dyne, and $k_{33} = 15.97\ 10^{-7}$dyne. (After Ref. 13)

following equation for the transverse phase change φ,

$$\gamma_1 \frac{\partial \varphi}{\partial t} - k_{11} \cos^2 \alpha \frac{\partial^2 \varphi}{\partial x^2} - k_{22} \frac{\partial^2 \varphi}{\partial y^2} + \frac{12\, k_{33}}{L^2} \varphi = \frac{2\pi L (n_e^2 - n_o^2)^2 \sin^2 \alpha \cos \alpha}{c n_e^4 \lambda} I, \tag{14}$$

where we have switched back to the frame having the z-axis along the beam ($\hat{x} = x/\cos\alpha$). In deriving Eq.(14) we used the z-profile of ϑ given by Eq.(12). Equation(14) can be compared now with Eq.(1) to obtain the actual values of the parameters τ, l_x, l_y and a. In particular, the diffusion lengths l_x and l_y are given

by

$$l_x = \frac{L}{2}\sqrt{\frac{k_{11}}{3k_{33}}}\cos\alpha$$
$$l_y = \frac{L}{2}\sqrt{\frac{k_{22}}{3k_{33}}} \qquad (15)$$

Because l_x depends on the beam incidence angle α, while l_y is a constant, we have perfect cylindrical symmetry in the (x,y)-plane ($l_x = l_y$) at the incidence angle $\bar{\alpha}$ given by $\cos\bar{\alpha} = \sqrt{k_{22}/k_{11}}$. For most liquid crystals $k_{22}/k_{11} \simeq 0.5$ and $\bar{\alpha} \simeq 45^0$.

EXPERIMENTS

Three different experiments have been carried out on optical self-organization with a single reflecting mirror. In all experiments a 50μm thick film of commercial nematic *E7* liquid crystal from *BDH* was used as Kerr optical medium. The glass walls enclosing the nematic film were coated with *HTAB* surfactant for homeotropic alignment. The sample was posed at oblique incidence into the beam of a cw Argon laser(λ=514nm), according to geometry (1). The beam spot size at the sample was reduced to $w = 250\mu$m and the light was linearly polarized in the incidence plane, in order to excite a pure extraordinary wave in the nematic film. After having traversed the liquid crystal (LC), the beam is backreflected by a "virtual mirror" [11], made by the two identical confocal lenses *L1* and *L2* (f = 50mm) and by the planar mirror *M1*, as shown in Fig.3. As the distance between *L1* and *L2* is $2f$, the system is equivalent to a "virtual mirror" *M1'* placed at distance $4f$ before *M1*, for any position of *M1*. That is, Fresnel propagation from the cell through that optical system and back is exactly equivalent to free space propagation to *M1'* and back. The overall reflectivity of our virtual mirror is about 60%. The lens *L3* and the microscope objective *MO* projected onto the screen *S* the near field image of the backward light after exiting the cell, for visual observation. In some experiments another lens and microscope objective were used to project the far field image. The use of the virtual mirror permits a great flexibility in the experiment: it can be positioned for example very close to the

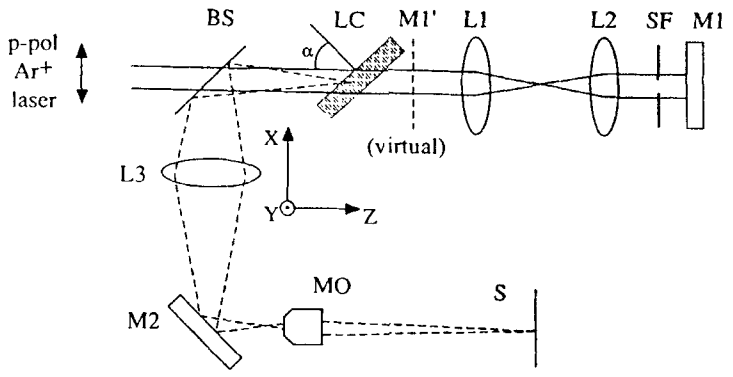

FIGURE 3 Experimental setup. M1, M2 mirrors; M1' virtual mirror; BS beam splitter; LC liquid crystal film; L1, L2 50mm focal-length lens; L3 lens; MO microscope objective; S screen.

sample without mechanical limitations and leaves enough room to insert optical devices (spatial filters, etc.), between the two lenses *L1* and *L2* in order to alter the feedback provided by the mirror *M1*. Moreover, the virtual mirror could be even moved across the sample, to reach "negative" mirror-to-sample distance d.

In the first experiment the spontaneous formation of hexagonal patterns was studied [9]. The spatial period Λ of the observed structure and the laser intensity threshold I_{th} were measured as a function of the mirror-to-sample distance d. In this experiment the laser incidence angle was 45^0, very close to the value $\bar{\alpha}$ for which cylindrical symmetry is recovered. The experimental results are shown in Figs.4 and 5. The curve (a) in Fig.5 is the ratio Λ/Λ_T as obtained from Firth's linearized theory. The curve (b) compares the experimental data (squares) for Λ/Λ_T with the line $\Lambda/\Lambda_T = 1$. In the curve (c) is plotted the quantity $(\pi^2/12)(\beta \sin\alpha/n_o)(I_{th}/I_{OFT})$, where I_{th} is the threshold for pattern formation as obtained from Firth's linearized theory, I_{OFT} is the threshold for the optical Fréedericksz transition at normal incidence, and β is given by Eq.(11). As we can see, the experimental data agree much better with Talbot's model rather than with the results obtained by the linear stability analysis of Firth's equation.

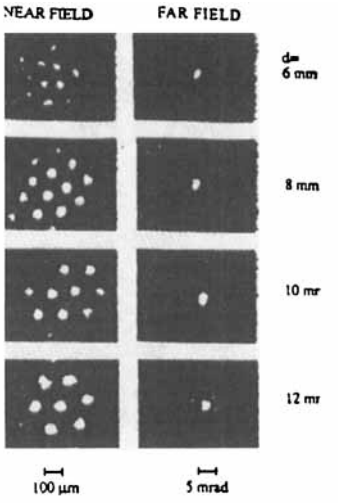

FIGURE 4 Pictures of the observed hexagonal patterns for various mirror-to-cell distance d. (a1-a2) far-field; (b1-b2) near-field. The liquid crystal was homeotropic nematic $E7$, 50μm thick. (After Ref. 9.)

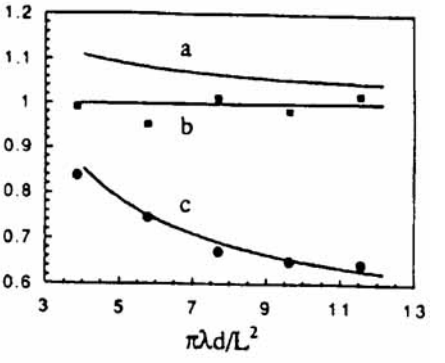

FIGURE 5 Hexagon lattice spatial period and threshold intensity for pattern formation as functions of the reduced mirror-to-sample distance $\pi\lambda d/L^2$ for a 50μm thick $E7$ homeotropic cell. Circles are the experimental data. The incidence angle was $\alpha = 45^0$.

In the second experiment, a virtual mirror at *negative* distance d from the liquid crystal cell was used, in this case the feedback field $u_1(x,y)$ can be obtained by back-propagating the field $u_0(x,y)$ [11]. Spontaneous formation of hexagonal structures was still obtained, but the relationship between the pattern spatial period Λ and the mirror-to-sample distance d was now different than in the previous case of positive distance d. This can be well understood in terms of Talbot model. From Fig.1, in fact, we see that positive feedback is obtained not only at $d = l_T/8$ as shown in Sec., but also at the *negative* value $d = -3l_T/8$, coresponding to a spatial period $\Lambda_T = 2\sqrt{-\lambda d/3}$. The measured period Λ of the hexagonal pattern as a function of the mirror-to-sample distance d is shown in Fig.6 both for positive and negative d. The agreement with the results of Talbot model is very good. The threshold power for the formation of the hexagonal pattern is reported in Fig.7, where the data are compared with the theory based on linear analysis for

a plane wave (dashed line) and for a beam having finite size (solid line). The threshold for finite size beams was found to increase with the absolute value of d. For a given spatial period of the pattern we have two values of d, but the absolute value of the negative distance is three times that of the positive, thus in the case of negative distance the threshold is much more affected by edge effects, as it is seen in Fig.7. As pointed out in Ref. 11, this experiment proves that the

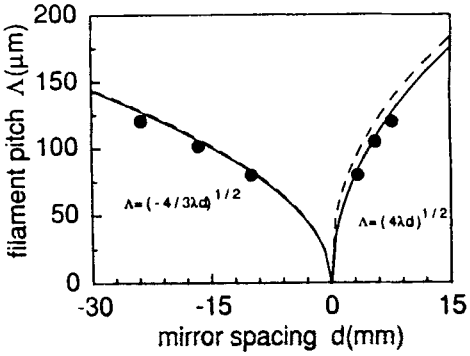

FIGURE 6 Spatial period of the hexagonal pattern vs. virtual mirror-to-cell distance: experimental (dots), theory based on Talbot effect (solid line) and theory from linear stability analysis (dashed line). (After Ref. 11.)

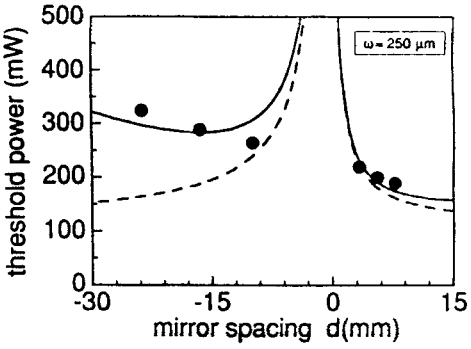

FIGURE 7 Threshold power for pattern formation vs virtual mirror-to-sample distance: experimental (dots), theory from linear stability analysis (dashed line), and linear stability theory accounting for the finite beam size (solid line). In the experiment, the beam waist at the sample was $w = 250\mu$m at $1/e^2$ intensity. (After Ref. 11.)

hexagons formation cannot be ascribed to the creation of *independent* filaments of light, due to self-focusing in the sample, as suggested, for example, in Ref. 23. As shown in Fig.8, converging rays from the liquid crystals, produced eventually by self-focusing, come back spread out over a larger area on the sample, in the case of

negative virtual mirror distance. In this case, any filament seed produced by self-focusing in the cell is cancelled out by the feedback due to the "negative" virtual mirror. We conclude, therefore, the hexagons are formed by a *collective* generation of filaments, such as the coherent superposition of three spatial gratings [11]. In our

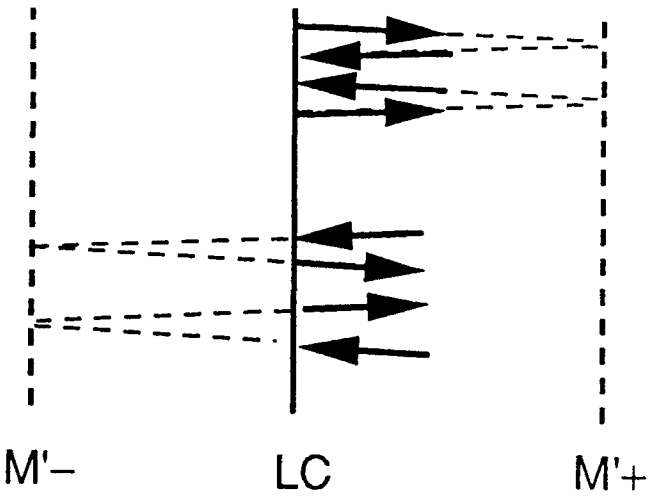

FIGURE 8 Converging rays from the liquid crystal sample come back either concentrated (for virtual mirror positive distance) or spread out (for virtual mirror negative distance).

third experiment [12], the overall cylindrical symmetry of the system was broken in order to observe the formation of patterns other than hexagons. As pointed out in the previous section, a way to break the cylindrical symmetry is introducing some amount of anisotropy by changing the beam incidence angle α. Because α affects only the diffusion length l_x and not l_y [see Eq.(16)], changing α alters the effective diffusion anisotropy of the sample. In our experiment the mirror distance d was adjusted to $d = 2mm$, so that the expected pattern period was $\Lambda \simeq 60\mu$m. The beam incidence angle was set to $\alpha = 70^0$, in order to have $l_x \simeq 5\mu$m, smaller that $l_y \simeq 10\mu$m . In this situation, rolls, rather than hexagons, were formed as shown in Fig.9. By lowering the incidence angle α, cylindrical symmetry is more and more restored and the pattern shows a transition from rolls to hexagons. A similar roll-to-hexagons transition was obtained by changing the mirror-to-cell dis-

tance d instead of the incidence angle α. In fact, as it easy to see from Eq.(5), once again this leads to a change in the anisotropy of the intensity threshold for pattern formation. In the same experiment, the effect of introducing a seed in

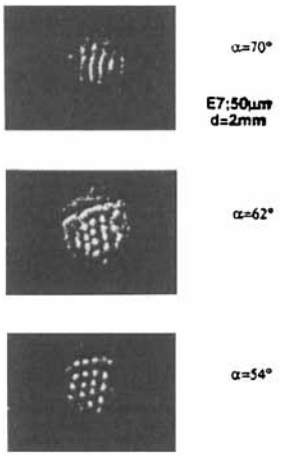

FIGURE 9 Near field pattern in the backward wave for d =2mm, $\alpha = 70^0$ (a), $\alpha = 62^0$ (b) and $\alpha = 54^0$ (c). The roll-to-hexagon transition is clearly visible. (After Ref. 12)

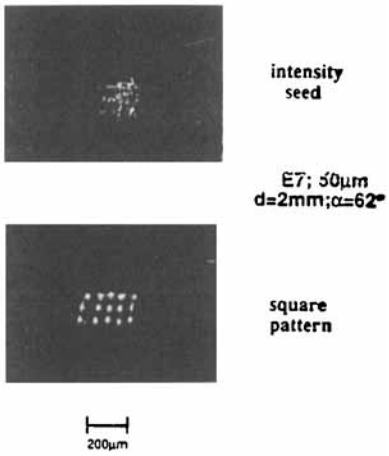

FIGURE 10 Observed near-field square pattern (a). The seed introduced by the slit (b). The pattern was obtained at $\alpha = 62^0$, $w = 250\mu$m, laser power $P = 430$mW.

the system feedback was also studied [11]. First, a vertical sharp blade was introduced next to the real backreflecting mirror. This produced the effect of forcing the hexagon orientation to have one side parallel to the blade edge. Rotating the blade produces a similar rotation in the observed hexagonal pattern. Second, we introduced a slit near the mirror. In this case and in the presence of some amount of diffusion anisotropy, the formation of square pattern was observed, as shown in Fig.10. The possibility to obtain square pattern was theoretically investigated by numerical simulation in Ref. 14. At the moment, no attempt was made to compare these numerical results with the experimental data.

CONCLUSIONS

In this paper we presented a series of experimental works on pattern formation and self-organization in liquid crystals, used as nonlinear Kerr optical media, obtained with a single backreflecting mirror as optical feedback. The results are in agreement with the numerical and theoretical results obtained by Firth, even if it seems that they could also be explained in terms of Talbot effect. In the experiments a virtual mirror was used, so that both positive and negative mirror-to-cell distances were studied. The case of negative distance is interesting, because it proves that the hexagonal pattern is due to a collective, rather than individual, filamentation of the laser beam in the nonlinear medium. Finally, we obtained patterns other than hexagons, i.e. rolls or squares, by introducing some amount of anisotropy in the sample effective diffusion lengths.

This work was carried out in the framework of an agreement between Fondazione Ugo Bordoni and the Italian P.T.Administration and under partial financial support from the National Research Council (CNR) in the frame of the Telecommunications Project. One of us (E.S.) acknowledges support from the special project MADOF by CNR and by Ministry of Scientific and Technologic Research.

REFERENCES

1. N.B.Abraham and W.J.Firth, J.Opt.Soc.Am., B7, 951 (1990);
2. M.Kreutzer, W.Balzer, and T.Tschudi, Appl. Opt., 29, 579 (1990);
3. F.T.Arecchi, G.Giacomelli, P.L.Ramazza, and S.Residori, Phys. Rev. Lett., 67, 3749 (1991);
4. G.D'Alessandro and W.J.Firth, Phys.Rev.Lett., 66, 2597 (1991);
5. G.A.Swartzlander,Jr., D.R.Andersen, J.J.Regan, H.Yin, and A.E.Kaplan, Phys. Rev. Lett., 66, 1583 (1991);
6. W.J.Firth, A.Fitzgerald, and C.Paré, J.Opt.Soc.Am., **B7**, 1087 (1990);
7. R.Macdonald and H.J.Eichler, Opt.Comm, 89, 289 (1992).

8. E.Santamato, M.Tamburrini, M.Bonavita, and S.Wabnitz, Digest of the Second Topical Meeting on Nonlinear Optics, August 17-21, Maui (Hawaii) (Optical Society of America, Washington, D.C., 1992), paper #TuB4.
9. M.Tamburrini, M.Bonavita, S.Wabnitz, and E.Santamato, Opt. Lett., 18, 855 (1993).
10. T.Honda, Opt.Lett., 18, 598 (1993).
11. E.Ciaramella, M.Tamburrini, and E.Santamato, Appl. Phys. Lett., 63, 1604 (1993);
12. E.Ciaramella, M.Tamburrini, and E.Santamato, Optics Letters, submitted.
13. E.Santamato, E.Ciaramella, and M.Tamburrini, Mol.Cryst.Liq.Cryst., 1993.
14. F.Papoff, G.D'Alessandrop, G.-L.Oppo, and W.J.Firth, Phys.Rev., A48, 634 (1993);
15. W.H.F.Talbot, Phyl.Mag., 9, 401 (1836);
16. Some reviews on nonlinear optics in liquid crystals have been appeared recently in the literature [Refs. 17,18,19,20];
17. N.V.Tabiryan, A.V.Sukhov, and B.Zel'dovich, The orientational optical nonlinearity of liquid crystals, Mol. Cryst. Liq. Cryst., 136, 1-140 (1986);
18. I.C.Khoo, Nonlinear optics of liquid crystals, Progress in Optics, XXVI, 107-161 (1988);
19. F.Simoni, Nonlinear optical phenomena in nematics, in Physics of liquid crystals, Gordon & Breach, N.Y. 1989;
20. see also the recent monography by I.C.Khoo and S.T.Wu, Optics and nonlinear optics of liquid crystals, Series in Nonlinear Optics, World Scientific, Singapore, 1993.
21. B.Ya.Zel'dovich, N.F.Pilipetskij, A.V.Sukhov, and N.V.Tabiryan, JEPT Lett., 32, 263 (1980);
22. S.D.Durbin, S.M.Arakelian, and Y.R.Shen, Phys. Rev. Lett., 47, 1411 (1981);
23. M.Markus, W.Balzer, and T.Tschudi, Appl.Opt., 29, 579 (1990);